UDK 669.721.5:621.791.763
Original scientific article/Izvirni znanstveni članek

ISSN 1580-2949
Mater. Tehnol.

PREPARATION OF Mg-6Zn AND A STUDY ON ITS RESISTANCE-SPOT WELDING MICROSTRUCTURE AND MECHANICAL PROPERTIES

PRIPRAVA ZLITINE Mg-6Zn TER ŠTUDIJ MIKROSTRUKTURE IN MEHANSKIH LASTNOSTI UPOROVNO TOČKOVNO VARJENIH SPOJEV

Dongqi Zhang[1], Zheng Jia[1,2*], Xiaowei Niu[2]

[1]College of Mechanical Engineering, Shenyang University, Shenyang 110044, China
[2]College of Environment, Liaoning Province Pollution Environmental Remediation Professional Technology Innovation Center & Shenyang Key Laboratory of Collaborative Technology Innovation for Industrial Pollution Reduction and Carbon Reduction, Shenyang University, Shenyang 110044, China

Prejem rokopisa – received: 2024-11-29; sprejem za objavo – accepted for publication: 2025-02-18

doi:10.17222/mit.2024.1348

This article investigates the effect of different welding currents on the microstructure, nugget diameter, and tensile strength of a 1.5-mm-thick Mg-6Zn magnesium alloy through resistance-spot welding. A detailed analysis is conducted using various experimental techniques, including tensile testing, microhardness testing, optical microscopy, and scanning electron microscopy. When the current is 16 kA, the hardness and peak value are 62.45 HV and 1.108 kN, respectively. Therefore, when the current is 16 kA, the hardness in the fusion zone is the smallest and the peak value and fusion diameter are the largest, which is the optimal spot-welding parameter. The welded joint is mainly composed of a fusion zone and a heat-affected zone. The microhardness of the fusion zone is the highest, significantly higher than that of the heat-affected zone and the base material. The fusion zone is mainly composed of equiaxed and columnar dendrites, and grain coarsening is observed in both the fusion zone and the heat-affected zone. There are two types of fracture modes for welded joints. When the size of the weld core is small, it is the joint surface fracture, and when the size of the weld core is large, it is the button fracture. We conducted in-depth research on the microstructure characteristics, fracture morphology, and microhardness distribution of the joint.

Key words: magnesium alloy, resistance-spot welding, welding joints, mechanical properties, microstructure

V članku avtorji opisujejo raziskavo vpliva različnih električnih tokov varjenja na mikrostrukturo, velikost in »lešnikasto« obliko navarka ter natezno trdnost spojev 1,5 mm debele pločevine iz magnezijeve zlitine tipa Mg-6Zn, ki so bili izdelani z uporovnim točkovnim varjenjem. Z detajlno analizo, ki je obsegala različne eksperimentalne tehnike (natezni preizkus, metalografske preiskave z optičnim in presevnim elektronskim mikroskopom, meritve mikro trdote) so določili vpliv parametrov varjenja. Pri električnem toku 16 kA je bila maksimalna izmerjena mikrotrdota 62,45 HV in natezna trdnost 1108 kN. Pri uporabi električnega toka 16 kA je bila v coni taljenja to najnižja izmerjena mikro trdota in velikost navarkov je bila največja, kar pa so optimalni zahtevani pogoji uporovnega točkovnega varjenja. Zvarni spoji so bili v glavnem sestavljeni iz cone taljenja in toplotno vplivane cone. Mikrotrdote v coni taljenja so bile v vseh primerih najvišje in višje od mikrotrdot izmerjenih v toplotno vplivani coni ter precej višje od mikrotrdote osnovnega materiala. Cono taljenja so v glavnem sestavljali grobi enakoosni in stebričasti dendriti. Rast kristalnih zrn je bila opažena v coni taljenja kot tudi v toplotno vplivani coni. Dva načina preloma zvarnih spojev so avtoriji opazili pri analizi pod SEM. Ko je bilo jedro zvara majhno je bila narava prloma krhka s vidnimi cepilnimi ploskvami. Ko pa je bila velikost jedra zvara velika, so imeli prelomi obliko gumba (iztrgan je bil zvarni spoj). Avtorji so v članku natančno opisali mikrostrukturne lastnosti, morfologijo prelomov in mehanske lastnosti zvarnih spojev izdelanih z uporovnim točkovnim varjenjem izbrane Mg zlitine.

Ključne besede: zlitina na osnovi magnezija, uporovno točkovno varjenje, zvarni spoji, mehanske lastnosti, mikrostruktura

1 INTRODUCTION

Magnesium and magnesium alloys are currently the lightest structural metal materials in industry, with a series of advantages such as high specific strength, good casting performance, and good electromagnetic shielding resistance. They are widely used in the aerospace, automotive, and 3C electronic product fields, playing an increasingly important role in achieving lightweight structural materials. They are known as the "most promising and competitive green metal structural materials of the 21st century".[1–3] However, the poor corrosion resistance, mechanical properties at room temperature, and poor weldability of magnesium alloys also limit their widespread application. In order to further improve the application range of magnesium alloys, the design and optimization of magnesium alloys have become a research hotspot.[4] In recent years, the development of high-performance magnesium alloys has attracted widespread attention.

Due to the special physical properties of magnesium alloys, it is difficult to obtain reliable joints during welding, and the welding of magnesium alloy structural components has become a technical key that restricts its ap-

*Corresponding author's e-mail:
jz140@163.com (Zheng Jia)

plication. The main problems of magnesium alloys during welding include oxidation, coarsening, porosity, etc. The current welding methods used for magnesium alloys include resistance-spot welding (RSW),[5] friction-stir welding (FSW),[6] electron-beam welding (EBW),[7] laser welding (LBW),[8] melting-and-inert-gas-shielded welding (MIG),[9] etc. Each welding method has certain specificity and limitations in practical welding applications. Resistance-spot welding is suitable for magnesium alloy thin plates rather than continuous connections. It is a welding method that uses the resistance heat generated by the current flowing through the welded part to locally melt the base material and form a joint.

Therefore, this study tested the weldability of a Mg-6Zn alloy through resistance-spot welding and determined the optimal process parameters based on the quality characteristics of the welded joints of Mg-6Zn magnesium alloy. The study was of the influence of different welding current parameters on the mechanical properties and microstructure characteristics of magnesium alloys, providing some basic information for future engineering applications.

2 EXPERIMENTAL METHODS

The preparation materials for the Mg-6Zn magnesium alloy in this experiment are the matrix-element magnesium (Mg) and the alloying-element zinc (Zn). The raw materials are: 99 % (*w*/%, the same below) magnesium ingots and 99 % zinc ingots. Magnesium alloy preparation is carried out using a crucible-type resistance furnace for alloy melting. Before melting, the rust on the inside of the steel mold is removed using sandpaper to ensure that there are no other alloy elements remaining inside the iron crucible used for melting. The iron crucible is then placed in a resistance furnace for heating to 500 °C, and pure magnesium blocks are placed to heat up to 735 °C. When it is completely melted and the temperature reaches 730 °C, turn off the temperature control power and open the melting furnace to scrape off the magnesium melt, then add zinc flakes, stir and keep warm for 20 min, and finally turn off the temperature control power. Then it was cast into the mold, and the chemical composition of the final as cast alloy was analyzed using inductively coupled plasma atomic emission spectroscopy (ICP-AES). **Table 1** lists the chemical composition of the experimental alloy.

Table 1: Chemical Composition Analysis of Mg-6Zn Magnesium Alloy (*w*/%)

Element	Zn	Mn	RE	Mg
Alloy composition	5.75	–	–	Balance

Remove the oxide layer and oil stains on the surface of the magnesium alloy to be welded before welding, and place it in anhydrous ethanol for ultrasonic cleaning and drying for later use. The experiment used an

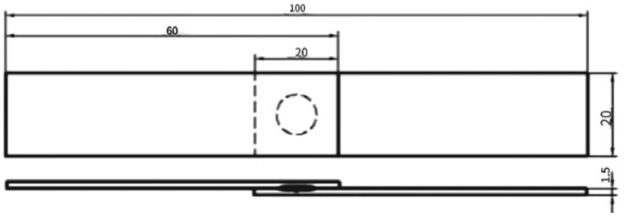

Figure 1: Schematic diagram of welding overlap

Yaskawa AC spot-welding robot for the welding, with copper selected for the electrodes. The experiment used an electrode pressure of 1 kN, welding time of 0.4 s, and welding currents of 12 kA, 14 kA, and 16 kA to weld the Mg-6Zn alloy. Performance testing was conducted on a microcomputer-controlled electronic universal testing machine, and the schematic diagram of the tensile specimen is shown in **Figure 1**. The stretching speed is 1mm/min, ensuring that the line of action of the tensile and shear forces passes through the center of the melt during loading. Cross cut the spot welded joint along the diameter direction of the welding point, and after embedding, grinding, and polishing, use a picric acid solution to corrode the microstructure of the welding point. Observe and analyze the microstructure of the fusion zone of the joint using an optical microscope and scanning electron microscope. The HX-1000TM/LCD digital microhardness tester was used to measure the microhardness of the fusion zone, heat-affected zone, and base metal of the sample after resistance-spot welding with three different welding currents. The fracture morphology and distribution were examined using SEM model S-4800.

3 RESULTS

3.1 The influence of welding current on the diameter of spot-welding nuggets

The formation of weld nuggets during resistance-spot welding largely determines the effective load-bearing area of the weld in the load-bearing structure.[10] **Figure 2**

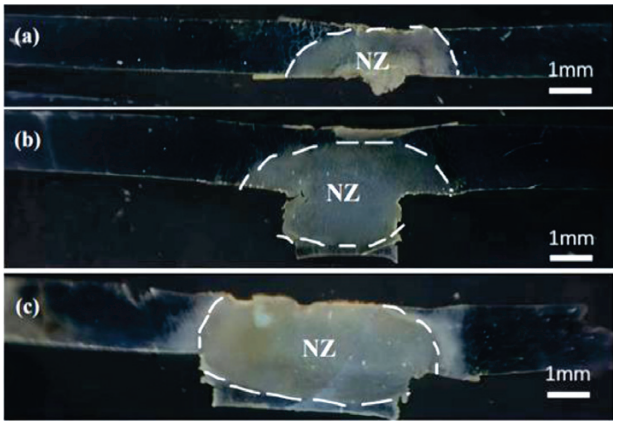

Figure 2: Macroscopic morphology of fusion nuclei under different welding currents: a) 12 kA, b) 14 kA, c) 16 kA

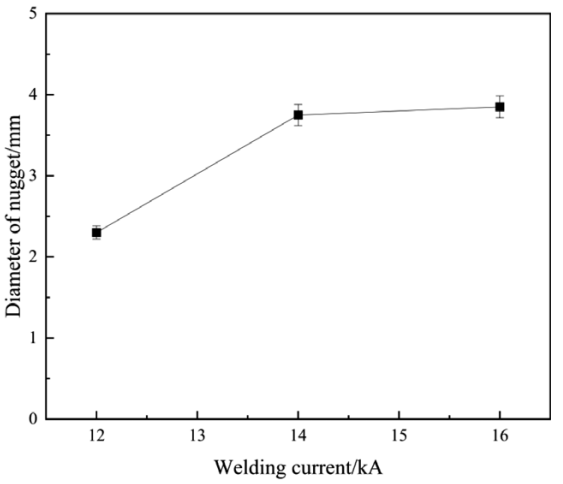

Figure 3: Effect of Welding Current on Nugget Diameter

shows the experimental results of the influence of welding current on the size of the weld nugget. It can be seen that the current of the welding machine has a significant impact on the size of the weld nugget. As the welding current increases, the size of the weld nugget increases. When the welding current increases from 12 kA to 16 kA. **Figure 3** show the diameter of the weld nugget increases from 2.3 mm to 3.85 mm, and the indentation depth of the joint increases. The heat source for resistance-spot welding is the resistance heat generated by the current passing through the welding area. As the welding current increases, the welding heat input also increases, resulting in an increase in the size of the weld nugget.[11]

3.2 Effect of Welding Current on Weld Seam Structure

The microstructure of the fusion zone determines the load-bearing capacity of the solder joint. **Figure 4** show, it can be seen that due to the different degrees of undercooling in different parts of the welded joint,[12] the microstructure of the welded joint obtained by resistance-spot welding Mg-6Zn magnesium alloy consists of three parts: the base metal (BM), the heat-affected zone (HAZ), and the fusion zone (NZ);[13] The fusion zone is mainly composed of columnar dendritic zone (CDZ) and equiaxed dendritic zone (EDZ) inside the fusion zone. There are significant differences in the microstructure between the spot welding area and other areas. The grains in this area are small and evenly distributed, and the grain distribution has a certain directionality. The results indicate that the welding current also has an impact on the microstructure of the weld nugget.[14]

As the current increases, the columnar dendritic region (CDZ) near the heat-affected zone becomes narrower and wider. When the welding current increases, the temperature in the fusion zone also rises, leading to an accelerated growth rate of columnar dendrites and an expansion of the columnar dendritic region. During resistance-spot welding, the temperature gradient and solute distribution in the fusion zone can affect the growth direction of crystals, leading to the formation of equiaxed dendrites. The size and morphology of the equiaxed dendrites can affect the performance of solder joints.[15,16]

As shown in **Figure 5**, for equiaxed dendrites (EDZ) in the fusion zone under different welding currents, when the current is 12 kA and the welding current is low, the

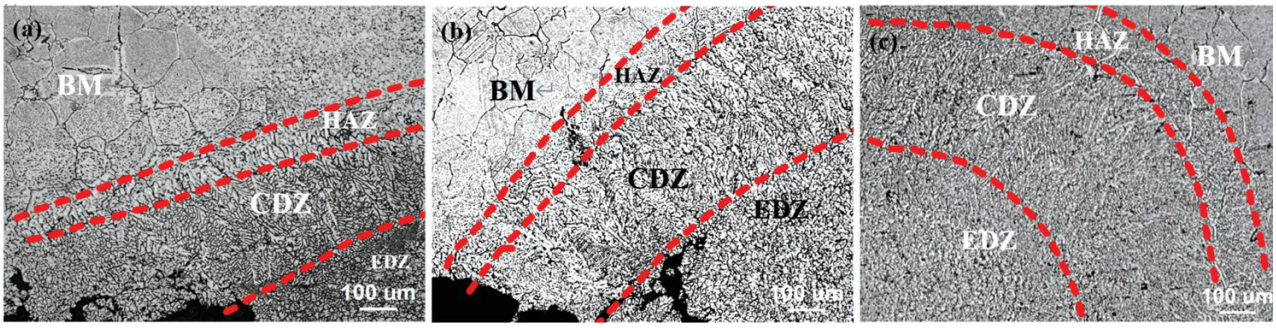

Figure 4: The overall morphology of spot-welding microstructure under different currents: a) 12 kA, b) 14 kA, c) 16 kA

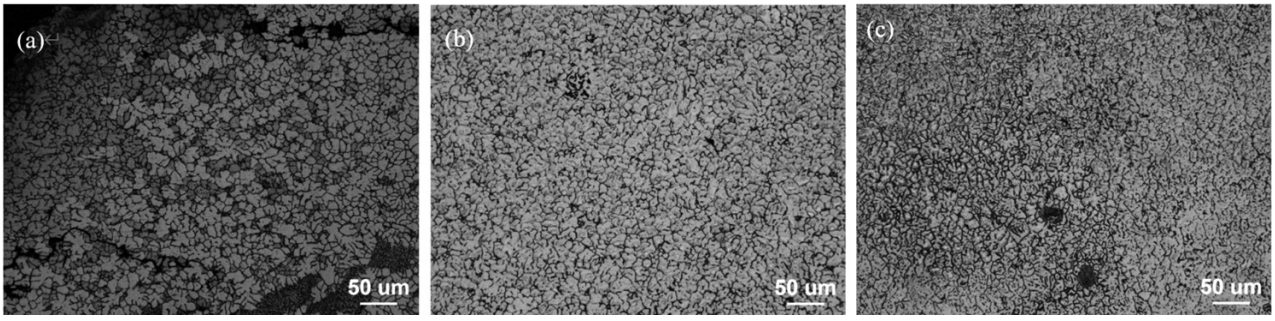

Figure 5: Isometric dendrites (EDZ) in the fusion zone under different welding currents: a) 12 kA, b) 14 kA, c) 16 kA

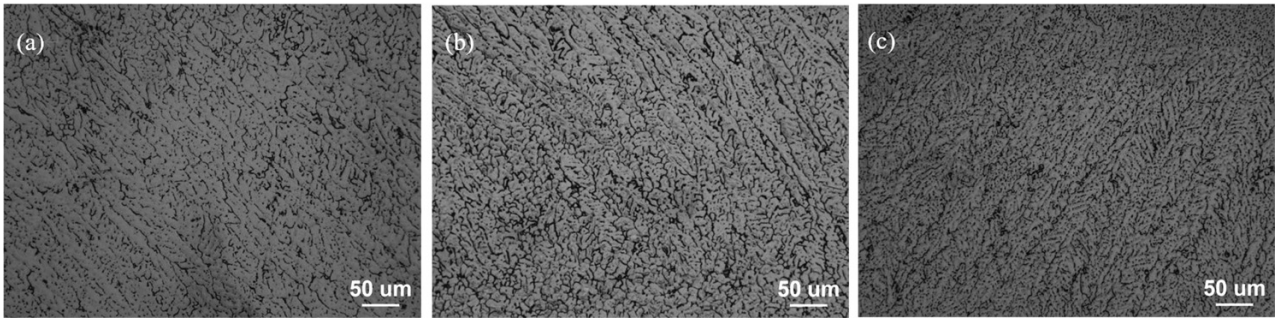

Figure 6: Columnar dendrites (CDZ) in the fusion zone under different welding currents: a) 12 kA, b) 14 kA, c) 16 kA

heat input is insufficient, resulting in incomplete formation of fusion nuclei in the weld joint and a relatively loose structure. When the current is 14 kA and 16 kA, the welding current gradually increases, the heat is sufficient, and the fusion zone is fully melted and crystallized, forming a relatively uniform equiaxed crystal structure. As the welding current increases, equiaxed dendrites become finer and more uniform. It can be concluded that as the current increases, the strength and toughness of the solder joint improve. At a welding current of 12 kA, the welding heat input is small, the nucleation time is short, and there is less melting of the base metal. It was found that the closer the grains are to the center of the fusion, the denser the grains. The area near the heat-affected zone solidifies first, and at the same time, heat dissipation is faster to form columnar dendrites.[17]

During spot welding, due to the passage of the welding current, the temperature at the welding point rapidly increases, causing the magnesium alloy to melt and form a molten pool.[18] During the solidification process of the melt pool, crystals begin to grow and form columnar dendrites. As shown in **Figure 6**, with the increase of welding current, the increase of heat causes the temperature gradient in the molten pool to increase, and the corresponding increase in undercooling is conducive to nucleation, leading to the formation of more crystal nuclei. The increase in the number of crystal nuclei makes the columnar dendritic crystals compete for space and resources during the growth process, limiting their growth and making the columnar dendritic grains smaller and smaller.[19] And more heat will accelerate the crystallization rate, shorten the crystal growth time, and also cause the columnar dendrites to solidify before they can fully grow.

The grains at the center of the fusion nugget change from columnar dendrites to equiaxed grains, and the grains become smaller and more uniform. The narrower the columnar dendritic zone (CDZ), the smaller the experimental force and the poorer the mechanical properties.

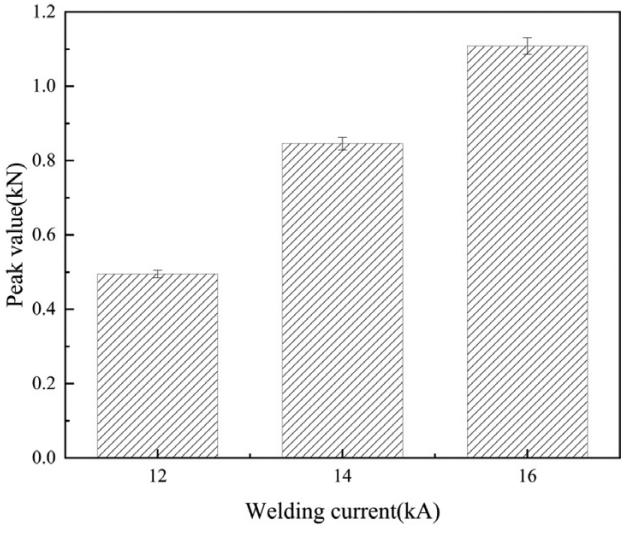

Figure 7: Changes in peak test force under different currents: a) 12 kA, b) 14 kA, c) 16 kA

3.3 Mechanical properties of resistance-spot welding joints

Different welding currents can lead to different nucleation diameters. Generally speaking, as the welding current increases, the nucleation diameter will also increase accordingly.[20] During the spot-welding process, the welding current generated when the electrode tip contacts the plate generates heat through the welded part, causing the joint to melt and form a fusion nugget.[21] When the welding current is low, the heat is not sufficient to completely melt the workpiece, resulting in a smaller diameter of the weld nugget. With the increase of welding current, the heat also increases, and the weldment can melt more fully, resulting in an increase in the diameter of the weld core. The diameter of the molten core with currents of 16 kA and 14 kA is larger than that of 12 kA. Install the six welded samples onto the tensile testing machine, ensuring that they are securely installed and well aligned. From **Figure 7** it can be seen that as the welding current increases from 12 kA to 14 kA and then to 16 kA, both the diameter of the weld core and the tensile mechanical properties gradually increase. When the diameter of the weld core is 2.3 mm, the tensile shear force of the joint is 0.495 kN. At a welding current of 14 kA, the diameter of the weld core is 3.75 mm, and the tensile shear force of the joint is

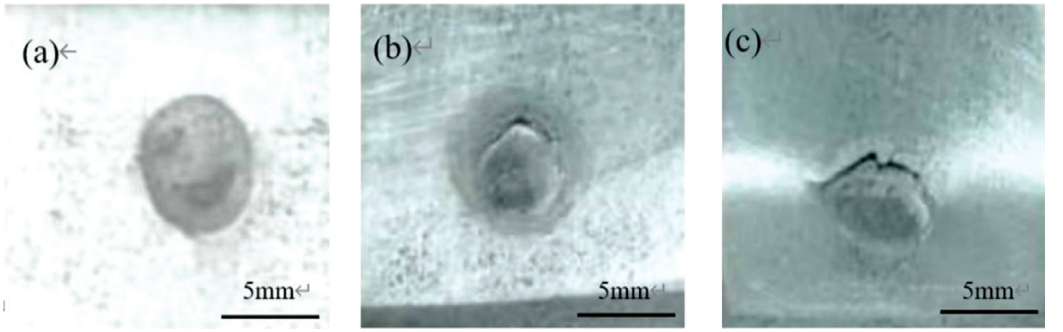

Figure 8: Macro appearance of the fracture: a) is interface failure, b) and c) are pull-out failures

0.864 kN. When the current is 16 kA, the diameter of the weld core is 3.85 mm, and the tensile shear force is 1.108 kN. In summary, it can be concluded that the diameter of the melt nugget is basically consistent with the change in tensile shear force.

3.4 Failure modes of resistance-spot welding joints

The characteristics of the failure modes of magnesium alloy spot-welding joints determine the degree of absorption and load-bearing capacity of the welded joints, which are generally divided into three types based on failure modes: interface failure, pull-out failure, and substrate tearing failure.[22] Among them, interface failure is a poor continuous failure mode, while substrate tearing failure is a better failure mode.[23]

The macroscopic morphology of the fracture surface is shown in **Figure 8**. From **Figure 8a**, it can be seen that the failure mode is interface failure when the spot-welding current is 12 kA.[24] When the heat input is small, joint surface fracture occurs because the size of the fusion core is small when the current is low, and the tensile and shear forces it can withstand are also low. When the applied stress exceeds the shear strength of the weld core, cracks rapidly propagate at the joint surface, and the spot welded weld core is separated from the joint surface, eventually forming a fracture at the joint surface.

Figures 8b and 8c show currents of 14 kA and 16 kA cause button fracture.[25] Due to the growth characteristics of the columnar crystal zone near the heat-affected zone, as stress continues to increase, the columnar dendrites become thinner, and their ability to resist deformation is relatively weak, which may quickly reach the fracture limit. Make it the weak surface of the fusion core and coincide with the plate seam in the high stress zone of the lap joint.[26] With the continuous action of external tensile and shear forces, cracks rapidly propagate along the melt nugget to the heat-affected zone and the base metal, causing the melt nugget to be pulled out of the base metal.

When the current is 12 kA and 14 kA, it can be observed from **Figure 9** that the fracture surface is rela-

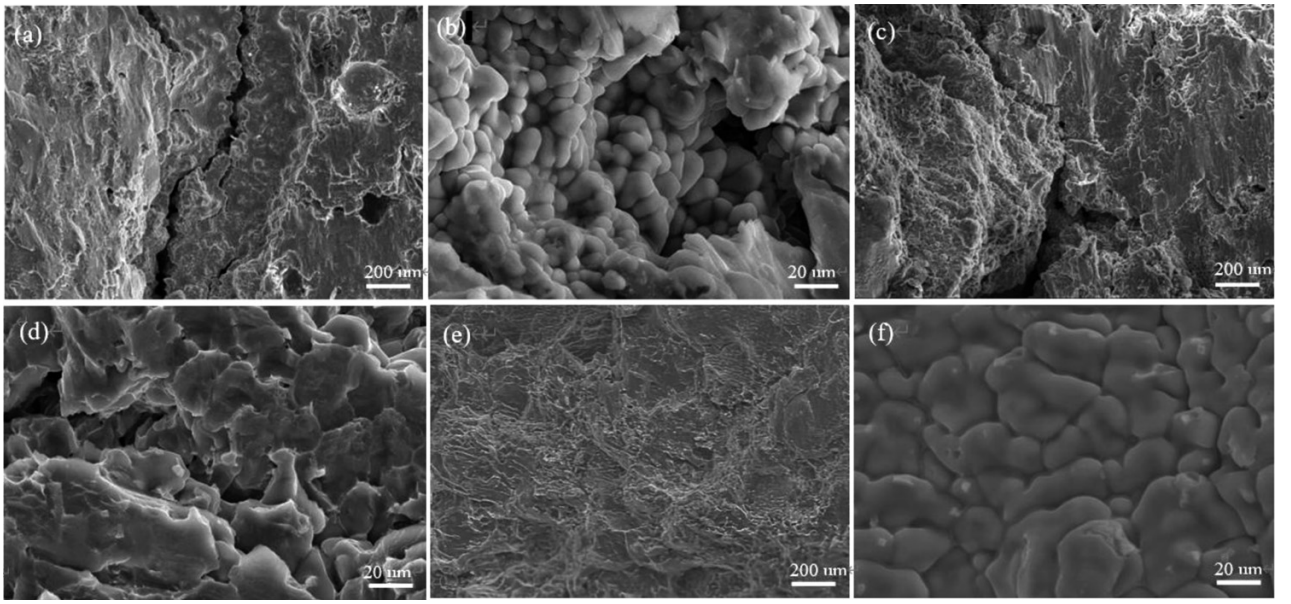

Figure 9: Fracture morphology diagram: (a) The fracture morphology of the joint surface under a current of 12 kA, b) The fracture morphology at high magnification, c) The fracture morphology of the joint under 14 kA current is similar to that under high magnification (d), e) The fracture morphology (f) of the joint surface under 16 kA current is the fracture morphology at high magnification

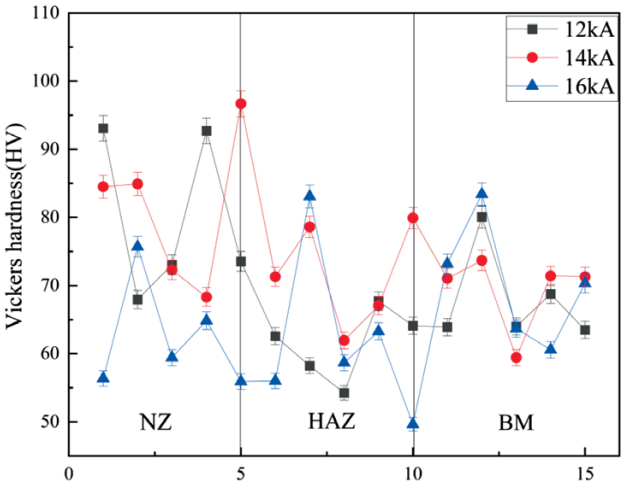

Figure 10: Hardness distribution map of different regions of the joint under different currents

tively flat and smooth with river like patterns, as well as some regular cleavage steps and small pores.[27] And there are cracks on the surface of the fracture, which is because it was pulled apart but not pulled, possibly due to other areas being more fragile. The fracture surface is perpendicular to the main tensile direction, and after the sample fractures, the residual deformation is very small, so it is a brittle fracture.

When the current is 16 kA, cleavage planes[28] can be observed from **Figure 9**, with some tearing edges appearing on the surface. The fracture surface is relatively rough, presenting a crystalline or granular appearance, and obvious grain boundary cracking marks can be seen. The grain boundaries appear relatively wide. So it is also brittle fracture. In summary, the fracture surfaces of spot-welded joints under different currents are all brittle fractures.

3.5 Hardness of spot-welded joints

The hardness value has good representativeness and repeatability. It has a wide range of applications in the research of metals, quality inspection, and evaluation of the heat-treatment effects. After spot welding, the microhardness of different micro regions varies, so the hardness values of the fusion zone, heat-affected zone, and base metal of the joint are tested separately. In the experiment, 5 points are selected for each micro region for testing, and the average value is taken as the hardness value of that region.

Due to the small indentation after spot welding of magnesium alloy, the damage to the sample is minimal.[29] So the Vickers hardness test was conducted on the sample. According to the test results in **Figure 10**, the average Vickers hardness values of the Mg-6Zn magnesium alloy in various regions are 80.07 HV, 61.38 HV, and 67.88 HV when the current is 12 kA. When the current is 14 kA, the average Vickers hardness of Mg-6Zn magnesium alloy in each region is 81.32 HV, 71.77 HV, and 69.38 HV. When the current is 16 kA, the average Vickers hardness of Mg-6Zn magnesium alloy in each region is 62.45 HV, 61.74 HV, and 70.33 HV. It can be seen that when the current is 16 kA, the hardness of the fusion zone is much lower than the other two groups.

4 CONCLUSIONS

This article focuses on the resistance-spot welding process of Mg-6Zn alloy with a thickness of 1.5 mm and analyzes and evaluates the effects of different currents on the nugget diameter, weld microstructure, and mechanical properties of spot welded joints. The following conclusions are drawn.

(1) Maximum nugget diameter: When the welding current is 16 kA, the nugget diameter reaches its maximum value of 3.85 mm. The variation of the nugget diameter is consistent with that of the tensile shear force.

(2) Optimal spot-welding parameters: When the welding current is 16 kA, the hardness of the nugget zone is the minimum, while the peak value and the nugget diameter are the maximum.

(3) Fracture mode: When the nugget size is small, the fracture occurs at the bonding surface; when the nugget size is large, button-type fracture occurs. Also, due to the action of the externally applied tensile shear force, the crack rapidly propagates from the nugget to the heat-affected zone and the base metal.

(4) The nugget zone is composed of equiaxed dendrites and columnar crystals. As the current increases, the grains become finer and more uniform.

Acknowledgements

The authors acknowledge the National College Students' Entrepreneurship Project 202311035033 the financial support from the Liaoning Province Natural Science Foundation Project of China(2023-MS-321) and the Liaoning Province International Cooperation Project (Project Number: 2023030491-JH2/107).

5 REFERENCES

[1] Y. Song, E. H. Han, D. Shan, D. Y. Shang, B.S. You, The effect of Zn concentration on the corrosion behavior of Mg–xZn alloys, Corros. Sci., 65 (**2012**), 322–330, doi:10.1016/j.corsci.2012.08.037

[2] Y. Hu, X. Guo, Y. Qiao, X. Wang, Q. Lin, Preparation of medical Mg-Zn alloys and the effect of different zinc contents on the alloy, J. Mater. Sci., 33 (**2022**) 1, 1–13, doi:10.1007/s10856-021-06637-0

[3] D. Y. Ding, Y. H. Du, M. F. Tang, B. Song, N. Guo, H. J. Zhang, S. F. Guo, Corrosion and discharge behavior of Mg-Zn-Mn-Nd alloys as primary Mg-air batteries anode, Trans. Nonferrous Met. Soc. China, 33 (**2023**) 7, 2014–2029, doi:10.1016/s 1003-6326(23)66240-5

[4] S. Nishimoto, M. Yamasaki, Y. Kawamura. Improving fracture toughness of rapidly solidified Mg-Zn-Y alloys by controlling precipitation of cluster-arranged nanoplates and LPSO phases, J. Alloy. Compd, 2014 (**2025**), 1014178720–178720, doi:10.1016/j.jallcom.2025.178720

[5] L. Liu, L. Xiao, J. C. Feng, The mechanisms of resistance spot welding of magnesium to steel, Metall Mater Trans A, 41 (**2010**), 2651–2661, doi:10.1007/s11661-010-0333-0

[6] S. M. Manladan, F. Yusof, S. Ramesh S,M. Fadzil, A review on resistance spot welding of magnesium alloys, Int J Adv Manuf Tech, 86 (2016), 1805–1825, doi:10.1007/s00170-015-8258-9

[7] S. Yang, B. Zhang. Experimental study of electron beam welding of magnesium alloys, Rare Metals, 30 (**2011**), 364–369, doi:10.1007/s12598-011-0304-7

[8] P. Leo, G. Renna, G. Casalino, A. G. Olabi, Effect of power distribution on the weld quality during hybrid laser welding of an Al–Mg alloy, Opt Laser Technol, 73 (**2015**), 118–126, doi:10.1016/j.optlastec.2015.04.021

[9] Z. Sun, D. Pan D, J. Wei, Comparative evaluation of tungsten inert gas and laser welding of AZ31 magnesium alloy, Sci. Technol. Weld. Join, 7 (**2022**) 6, 343–351, doi:10.1179/136217102225006831

[10] S. M. Hassoni, O. S. Barrak, M.I. Hussein Ismail, S.K. Hussein. Effect of Welding Parameters of Resistance Spot Welding on Mechanical Properties and Corrosion Resistance of 316L, JMR, 25 (**2022**), e20210117, doi:10.1590/1980-5373-mr-2021-0117

[11] T. Xu, Y. Yang, X. Peng, J. Song, F. Pan. Overview of advancement and development trend on magnesium alloy,. J. Magnes. Alloy, 7 (**2019**) 3, 536–544, doi:10.1016/j.jma.2019.08.001

[12] J. Kubasek, D. Vojtěch, Structural characteristics and corrosion behavior of biodegradable Mg–Zn, Mg–Zn–Gd alloys, J. Mater. Sci, 24 (**2013**), 1615–1626, doi:10.1007/s10856-013-4916-3

[13] A. Macwan, D. L.Chen, Ultrasonic spot welding of rare-earth containing ZEK100 magnesium alloy to 5754 aluminum alloy, Mater. Sci. Eng.A, 666 (**2016**), 139–148, doi:10.1016/j.msea.2016.04.060

[14] S. M. Manladan, F. Yusof, S. Ramesh, M. Fadzil, A review on resistance spot welding of magnesium alloys, Int. J. Adv. Manuf. Technol., 86 (**2016**), 1805–1825, doi:10.1007/s00170-015-8258-9

[15] A. Hasanniah, M. Movahedi, Welding of Al-Mg aluminum alloy to aluminum clad steel sheet using pulsed gas tungsten arc process, J. Manuf. Process, 31 (**2018**), 494–501, doi:10.1016/j.jmapro.2017.12.008

[16] G. Song, T. Li, L. Chen, The mechanical properties and interface bonding mechanism of immiscible Mg/steel by laser–tungsten inert gas welding with filler wire, Mater. Sci. Eng.A, 736 (**2018**), 306–315, doi:10.1016/j.msea.2018.08.078

[17] D. Zander,N. A. Zumdick, Influence of Ca and Zn on the microstructure and corrosion of biodegradable Mg–Ca–Zn alloys, Corros. Sci., 93 (**2015**), 222–233, doi:10.1016/j.corsci.2015.01.027

[18] A. Singh, S. P. Harimkar, Laser surface engineering of magnesium alloys: a review, Jom, 64 (**2012**), 716–733, doi:10.1007/s11837-012-0340-2

[19] Y. Li, S. Arthanari, Y. Guan, Influence of laser surface melting on the properties of MB26 and AZ80 magnesium alloys, Surf. Coat. Technol, 378 (**2019**), 124964, doi:10.1016/j.surfcoat.2019.124964

[20] Y. C. Guan, W. Zhou, H. Y. Zheng, Effect of laser surface melting on corrosion behaviour of AZ91D Mg alloy in simulated-modified body fluid, J. Appl. Electrochem, 39 (**2009**), 1457–1464, doi:10.1007/S10800-009-9825-2

[21] S. Y. Liu, J. D. Hu, Y. Yang, Z. X. Guo, H. Y. Wang, Microstructure analysis of magnesium alloy melted by laser irradiation, Appl. Surf. Sci, 252 (**2005**) 5, 1723–1731, doi:10.1016/J.APSUSC.2005.03.110

[22] X. Cao, M. Jahazi. Effect of welding speed on the quality of friction stir welded butt joints of a magnesium alloy, Mater. Des, 30 (**2009**) 6, 2033–2042, doi:10.1016/J.MATDES.2008.08.040

[23] G. Padmanaban, V. Balasubramanian, An experimental investigation on friction stir welding of AZ31B magnesium alloy, Int. J. Adv. Manuf. Technol, 49 (**2010**), 111–121, doi:10.1007/s00170-009-2368-1

[24] Z. Zhang, L. Liu, S. Gang, Welding characteristics of AZ31B magnesium alloy using DC-PMIG welding, T NONFERR METAL SOC, 23 (**2013**) 2, 315–322, doi:10.1016/S1003-6326(13)62463-2

[25] M. Jafarian, A. Khodabandeh, S. Manafi, Evaluation of diffusion welding of 6061 aluminum and AZ31 magnesium alloys without using an interlayer, Mater. Des (**2015**) 65, 160–164, doi:10.1016/j.matdes.2014.09.020

[26] M. Wahba, S. Katayama, Laser welding of AZ31B magnesium alloy to Zn-coated steel, Mater. Des, 35 (**2012**), 701–706, doi:10.1016/J.MATDES.2011.10.031

[27] P. Carlone, G. S, Palazzo,Characterization of TIG and FSW weldings in cast ZE41A magnesium alloy, J. Mater. Process. Technol, 215 (**2015**), 87–94, doi:10.1016/j.jmatprotec.2014.07.026

[28] X. Qi, G. Song, Interfacial structure of the joints between magnesium alloy and mild steel with nickel as interlayer by hybrid laser-TIG welding, Mater. Des, 31 (**2010**) 1, 605–609, doi:10.1016/j.matdes.2009.06.043

[29] G Song, Z Diao, X Lv, L Liu, TIG and laser–TIG hybrid filler wire welding of casting and wrought dissimilar magnesium alloy, J. Manuf. Process, 34 (**2018**) 204–214, doi:10.1016/j.jmapro.2018.06.005